This article was downloaded by: [University of California, San Diego]
On: 11 August 2012, At: 10:35
Publisher: Taylor & Francis
Informa Ltd Registered in England and Wales Registered Number: 1072954
Registered office: Mortimer House, 37-41 Mortimer Street, London W1T 3JH, UK

Molecular Crystals and Liquid Crystals

Publication details, including instructions for authors and subscription information:
http://www.tandfonline.com/loi/gmcl20

Modelling of the Formation of Non-Uniform Polymer Networks in Devices

N. Dessaud [a] & E. P. Raynes [a]

[a] Department of Engineering Science, University of Oxford, Oxford, UK

Version of record first published: 18 Oct 2010

To cite this article: N. Dessaud & E. P. Raynes (2004): Modelling of the Formation of Non-Uniform Polymer Networks in Devices, Molecular Crystals and Liquid Crystals, 410:1, 475-485

To link to this article: http://dx.doi.org/10.1080/15421400490433523

PLEASE SCROLL DOWN FOR ARTICLE

Full terms and conditions of use: http://www.tandfonline.com/page/terms-and-conditions

This article may be used for research, teaching, and private study purposes. Any substantial or systematic reproduction, redistribution, reselling, loan, sub-licensing, systematic supply, or distribution in any form to anyone is expressly forbidden.

The publisher does not give any warranty express or implied or make any representation that the contents will be complete or accurate or up to date. The accuracy of any instructions, formulae, and drug doses should be independently verified with primary sources. The publisher shall not be liable for any loss, actions, claims, proceedings, demand, or costs or damages

whatsoever or howsoever caused arising directly or indirectly in connection with or arising out of the use of this material.

Downloaded by [University of California, San Diego] at 10:35 11 August 2012

Mol. Cryst. Liq. Cryst., Vol. 410, pp. 475/[1003]–485/[1013], 2004
Copyright © Taylor & Francis Inc.
ISSN: 1542-1406 print/1563-5287 online
DOI: 10.1080/15421400490433523

Downloaded by [University of California, San Diego] at 10:35 11 August 2012

MODELLING OF THE FORMATION OF NON-UNIFORM POLYMER NETWORKS IN DEVICES

N. Dessaud and E. P. Raynes†*
Department of Engineering Science, University of Oxford, Parks Road, Oxford, OX1 3PJ, UK

Polymer Stabilised Liquid Crystal (PSLC) devices contain a polymer network (PN) formed from a liquid crystal host containing a low concentration of reactive liquid crystalline monomers. If a strongly UV absorbing liquid crystal is used, the UV intensity profile during polymerisation creates a non-uniformity in the polymerisation process and the final polymer distribution across the cell [1]. A theoretical model of the polymerisation process of the reactive mesogen molecules is presented which takes into account the UV intensity profile, the rate of polymerisation and molecular diffusion. The PN distribution has been calculated using realistic reaction parameters, diffusion constants and UV absorption coefficients for both a UV absorbing (E7) and a non-absorbing (ML1001) liquid crystal. SEM observations and optical microscopy were carried out and are found to support the numerical predictions.

Keywords: diffusion; evanescent wave; observations; polymerisation reaction; PSLCDs

1. INTRODUCTION

In Polymer Stabilised Liquid Crystal (PSLC) devices, a polymer network has been formed from a liquid crystal host containing a low concentration of reactive liquid crystalline monomers, referred to as reactive mesogens (RMs). The presence of this 3-dimensional polymer network influences the device's static and dynamic switching properties [2,3].

The authors thank Drs Paul Bonnett and Zabbie Acosta for their help and advice throughout the course of this study. Drs Steve Elston is thanked for his ideas and contribution on the evanescent optical studies and Dr Brendan Poole for his help on the SEM observations. Sharp Laboratories of Europe, Ltd and EPSRC are thanked for funding ND as well as Merck Specialty Chemicals Ltd for supplying materials.

Address correspondence to N. Dessaud, Department of Engineering Science, University of Oxford, Parks Road., Oxford, OX1 3PJ, UK. E-mail: nathalie.dessaud@eng.ox.ac.uk
†E-mail: peter.raynes@eng.ox.ac.uk

Downloaded by [University of California, San Diego] at 10:35 11 August 2012

Several groups have modelled the effect of the PN on the device electro-optic properties [4–6]. Hoke [5] introduced the possibility of a non-uniform PN concentration across the cell thickness arising from the attraction of activated molecules to the two surfaces. However, the UV absorbing liquid crystals used in reference 1 showed a PN concentration distribution not symmetric around the cell centre. This was shown quite simply by filling the gap between two glass plates with an RM/LC mixture, exposing it to UV to initiate the PN formation, separating both glass plates and washing the LC away using pentane. On the side nearer the UV source a significant quantity of PN was formed, whereas there was almost none on the other side. Therefore, any surface attraction effect, has to be coupled with another effect; this was suggested as the UV absorption coefficients of the liquid crystal material [1]. Modelling the polymerisation process should give some indication of the PN distribution to be expected and may allow a better understanding of the effect of the PN on the cell switching properties.

When reactive mesogen molecules are mixed with UV absorbing liquid crystal molecules, the resulting UV intensity profile leads to a difference in the activation of the photoinitiator molecules and creates non-uniformity in the polymerisation process. The polymerisation of reactive mesogen molecules in the liquid crystal cell has been modelled by taking into consideration the UV intensity distribution, the rate of polymerisation of the RM molecules and their molecular diffusion using a standard one-dimensional diffusion equation. Similar equations describing the formation of holographic diffraction gratings and polymer networks can be found in references 7, 8, 9 and 10. The first part of this paper describes the diffusion/photopolymerisation model proposed together with some predictions of the expected PN distributions as a function of the cell thickness and RM concentration. We checked qualitatively our predictions using SEM observations on 5 μm cells for absorbing and non-absorbing LCs and quantitatively by observing the network formed in twisted nematic structures for different cell thickness, RM concentrations and LCs. An attempt to use evanescent optics to observe directly the PN profile is also described.

2. THE DIFFUSION/PHOTOPOLYMERISATION MODEL

a) Principle

The polymer network is formed by a free radical polymerisation [11] based on the absorption of photons by the photosensitive photoinitiator molecules introduced in small quantities to the RM/LC mixture. The photoinitiator forms radicals when exposed to light in its absorption region [12], and these initiate the reaction.

Downloaded by [University of California, San Diego] at 10:35 11 August 2012

If the liquid crystal is absorbing at the UV wavelength λ_0 used to initiate the polymerisation, an intensity profile *I(z)* appears through the cell thickness inducing a non-uniform polymerisation mechanism with the PN forming faster in the areas with higher illumination. If A is the absorption coefficient of the LC/RM/PI mixture, the light intensity profile *I(z)* can be found from the Beer-Lambert law (Eq. (1)).

$$I(z) = I_0 10^{-Az} \tag{1}$$

This non-uniform intensity through the cell thickness induces a gradient in the concentration of un-reacted molecules leading to diffusion to the less concentrated areas. Both mechanisms (reaction and diffusion) need to be included to understand the PN formation mechanism. The theoretical rate of polymerisation R_p can be found from the polymerisation process (Eq. (2)) and is dependent on the polymerisation constants of propagation k_p and termination k_t, the photoinitiator efficiency Φ_i, the monomer concentration $[M]$ and the number of photons absorbed n_{photons} [12,13].

$$\mathrm{R_p} = \mathrm{k_p[M]}\left(\frac{\Phi_\mathrm{i}\mathrm{n_{photons}}}{\mathrm{k_t}}\right)^{1/2} \tag{2}$$

The number of photons absorbed is given by Eq. (3), where h is Plank's constant, c the velocity of light in vacuum, ε_{PI} the molar extinction coefficient of the photoinitiator molecules and c_{PI} their concentration.

$$\mathrm{n_{photons}(z)} = \frac{\lambda_0}{\mathrm{hc}}\ \ln 10\, \varepsilon_{\mathrm{PI}} \mathrm{c_{PI}} \mathrm{I(z)} \tag{3}$$

Before the polymerisation starts, a homogeneous mixture is present in the cell. *u(z,t)* and *v(z,t)* are respectively the monomer and polymer concentrations at position z and time t after the start of the UV exposure. $[\mathrm{RM}]_0$ is the initial concentration of RM.

If a section δz is considered, the change in the number of RM molecules is the sum of their consumption during polymerisation (Eq. (4)) and their diffusion to less concentrated areas. The PN does not diffuse, so the change in *v(z,t)* is due only to its formation during polymerisation (Eq. (5)).

$$\frac{\partial u(z,t)}{\partial t} = D_0 \frac{\partial}{\partial z}\left[\frac{\partial u(z,t)}{\partial z}\right] - K u(z,t) 10^{-AZ/2} \tag{4}$$

$$\frac{\partial v(z,t)}{\partial t} = K u(z,t) 10^{-A.Z/2} \quad \text{and} \quad A = \sum \varepsilon_i c_i \tag{5}$$

where $K = K_1 K_2 K_3$. $K_1 = \sqrt{\lambda_0 I_0}$, $K_2 = \sqrt{\frac{k_p^2 \Phi_i \varepsilon_{PI} c_{PI}}{k_t}}$, $K_3 = \sqrt{\frac{\ln(10)}{\mathrm{Nh\,c}}}$.

K_1 depends on the exposure conditions, K_2 on the material properties and concentrations, and K_3 is a constant. The following boundary conditions are considered:

$$u(z,0) = RM_0, \quad \text{for } 0 \leq z \leq d$$

$\frac{\partial u(z,t)}{\partial z}|_{z=0} = 0$ and $\frac{\partial u(z,t)}{\partial z}|_{z=d} = 0$ for $0 \leq t < \infty$ (no flux at the surfaces).

Downloaded by [University of California, San Diego] at 10:35 11 August 2012

b) PN Distribution

The strongly absorbing LC host modelled is the LC mixture E7. The UV source emits light with intensity $I_0 = 1\,\mathrm{mW/cm^2}$ at a wavelength around $\lambda_0 = 365\,\mathrm{nm}$ specific absorption parameters have been taken from literature or measured:

$$\varepsilon_{\mathrm{pi}} \sim 1000\,\mathrm{m^3 \cdot mol^{-1} \cdot m^{-1}},\ \varepsilon_{\mathrm{LC}} \sim 100\,\mathrm{m^3 \cdot mol^{-1} \cdot m^{-1}},$$
$$\varepsilon_{\mathrm{RM}} \sim 0\,\mathrm{m^3 \cdot mol^{-1} \cdot m^{-1}}.$$

The diffusion constant D_0 is taken as constant in time. Approximate typical values for K and D_0 are $1\,\mathrm{s^{-1}}$ and $10^{-10}\,\mathrm{m^2\,s^{-1}}$ respectively. Several cells using 1, 2, 3 and 5% RM in either very absorbent ($\varepsilon_{\mathrm{E7}} \sim 300\,\mathrm{m^3 \cdot mol^{-1} \cdot m^{-1}}$) or non-absorbent ($\varepsilon_{\mathrm{ML1001}} \sim 0\,\mathrm{m^3 \cdot mol^{-1} \cdot m^{-1}}$) LCs were modelled and their final PN distribution plotted in 2 and 10 μm gap cells (Fig. 1).

Absorbing LCs in thick cells give a less uniform PN distribution than thin cells and non-absorbing LCs.

3. SEM OBSERVATIONS

For making SEM observations, the samples were prepared according to Figure 2. The filled cell was exposed to UV light using a 1-sided exposure and the liquid crystal and un-reacted RM washed away by immersion in toluene for several days. The cell was then prepared for observation in the SEM by coating with gold. Both exposed and non-exposed plates were cut in order to allow 3 different observations: gap, exposed side and non-exposed side views.

For the UV absorbing LC material (E7), there is a clear difference in PN density on the exposed side and non-exposed one. This difference is reduced when the non-absorbing LC material (ML1001) is used and, in most cases (1, 2 and 5% RM257 in ML1001), the structures look very

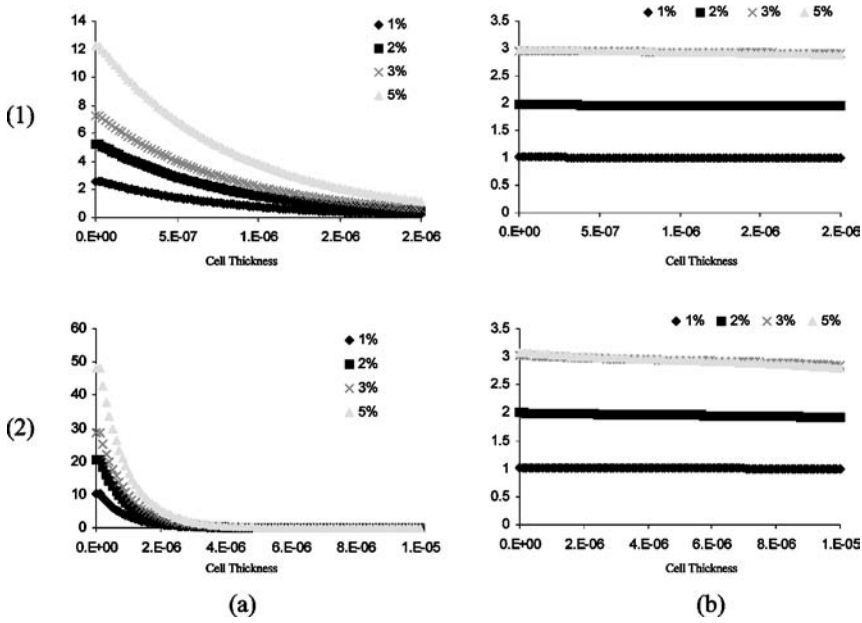

FIGURE 1 PN distribution profile in % as a function of the initial RM concentrations. Different cell thicknesses ((1) 2 μm and (2) 10 μm) and for (1) absorbing and (2) non-absorbing LCs.

similar. The structural differences on exposed and non-exposed surfaces are directly linked to the LC UV absorption, and can be observed over the whole concentration range of 1 to 5% studied (Fig. 3).

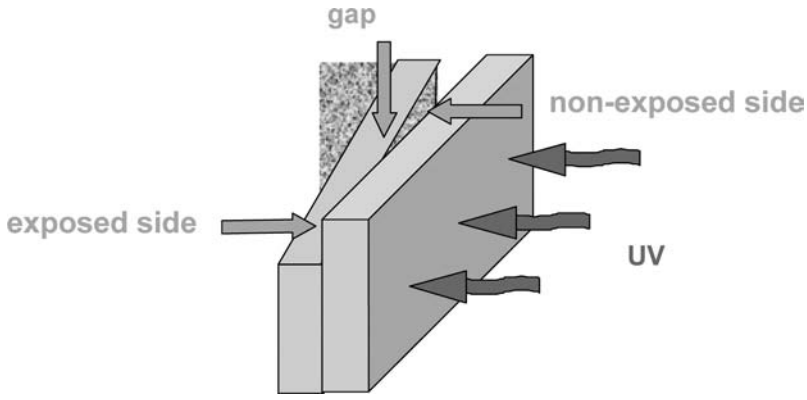

FIGURE 2 SEM observations.

Downloaded by [University of California, San Diego] at 10:35 11 August 2012

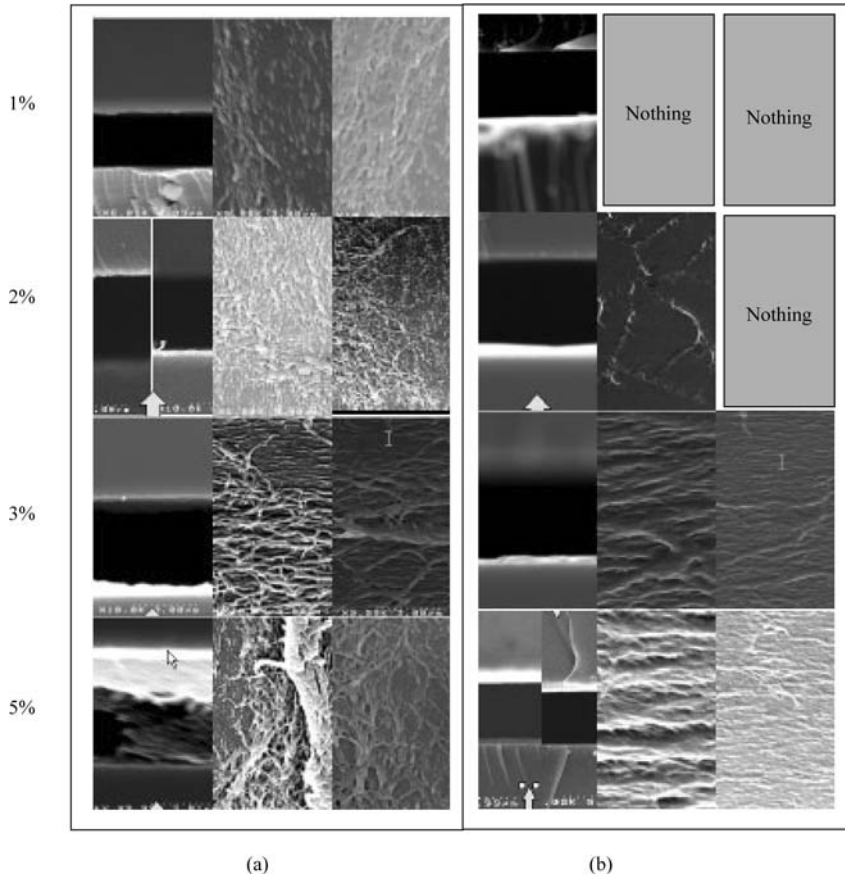

FIGURE 3 SEM pictures for (a) ML1001 and (b) E7 with different RM concentrations (1%, 2%, 3% and 5%). For each LC and each concentrations: picture 1: gap – picture 2: exposed side and picture 3: non-exposed side observations.

For a low RM concentration in E7, the absence of PN and the strange structure obtained for respectively the 1 and 2% mixtures compared with the 3 and 5% mixtures, suggests that the immersion in toluene may have damaged or even destroyed the initial PN structure.

As the network becomes denser, the network can be seen all the way across the cell. The network may not have been so damaged by the toluene because it is denser and therefore stronger, whereas lower concentration networks can be easily damaged. The difference in fibre sizes observed for a 5% RM in ML1001 may be explained by the concept of fractal growth of polymer [14].

Downloaded by [University of California, San Diego] at 10:35 11 August 2012

Because the polymer network is not observed *in-situ*, the observations made have to take into account possible damage to the initial network structure.

4. OBSERVATIONS USING A POLARISING MICROSCOPE

Following the experimental procedure in reference 1, some observations were carried out with the liquid crystal host still present by studying the optical properties of twisted nematic layers. Several cell thickness were studied (2, 5 and 10 μm) using different RM concentrations in the range 1 to 5% in both absorbing (E7) and non-absorbing (ML1001) liquid crystals.

A UV exposure of 1 mW/cm^2 at around 365 nm was carried out in the liquid crystal phase at room temperature for 15 minutes on each sample with the exposed side marked. The samples were then observed at 65°C (above the nematic-isotropic transition temperature of both liquid crystals). The cells were placed between crossed polarisers so that the input director of the TN cell is parallel to the optical axis of the first polariser. The cell was then rotated away from this initial position and a series of minimum and maximum transmissions were observed. The amount of light transmitted though a cell as it is rotated between crossed polarisers was calculated using numerical modelling based on the Jones matrix [15] assuming a linear dependence between the local PN concentration and the residual birefringence present. The angle for minimum transmission is measured. Both experimental results (Fig. 4) and numerical calculations (Fig. 5) are presented for E7 and ML1001.

For ML1001, the angles of minimum transmission θ_{Tmin} are scattered around 45°, which agrees with the predictions for a non-absorbing LC (Fig. 5d).

For the UV absorbing E7, θ_{Tmin} is close to $+/-30°$ for most RM concentrations. We can conclude that the PN is not uniformly distributed. Thicker cells seem slightly less uniformly distributed, but the differences observed between different cell thicknesses were expected to be bigger. This might be explained by a dependency of the diffusion parameter with the local PN concentration, which was not included in this model.

For 2, 5 and 10 μm cells, the extinction angle does not vary as the RM concentration is increased above 2% in E7. This seems to agree with the PN formation model, as a change in RM concentration influences only slightly the network profile (Fig. 5). However, the prediction for the 1% mixture does not agree with the experiment. Here the network is very weak and most of the time, it is quite hard to measure the extinction angle due to a low average birefringence. This may arise because during the formation process for very low RM concentrations the molecules may have problems reacting with each other as a result of their low concentration.

Downloaded by [University of California, San Diego] at 10:35 11 August 2012

Downloaded by [University of California, San Diego] at 10:35 11 August 2012

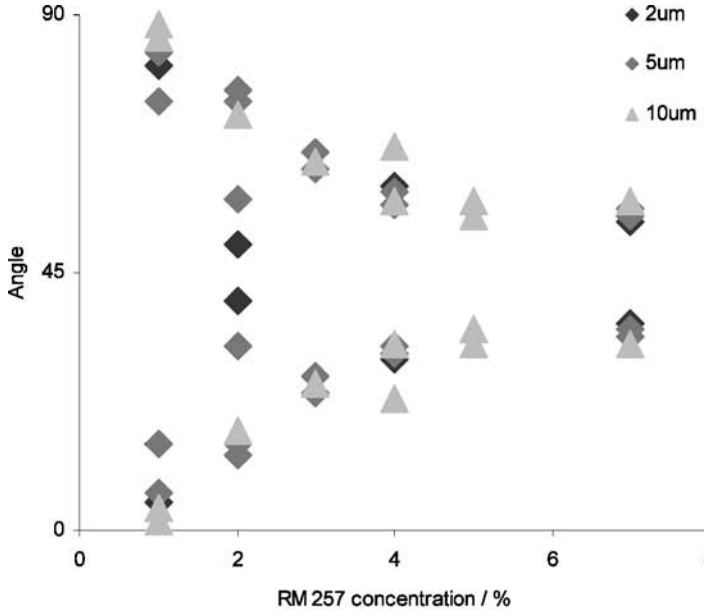

(a)

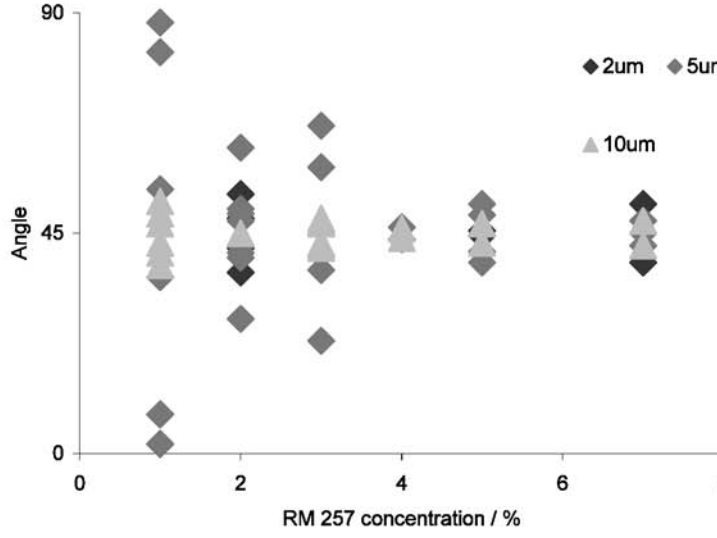

(b)

FIGURE 4 Experimental results for different cells (a) E7 (b) ML1001.

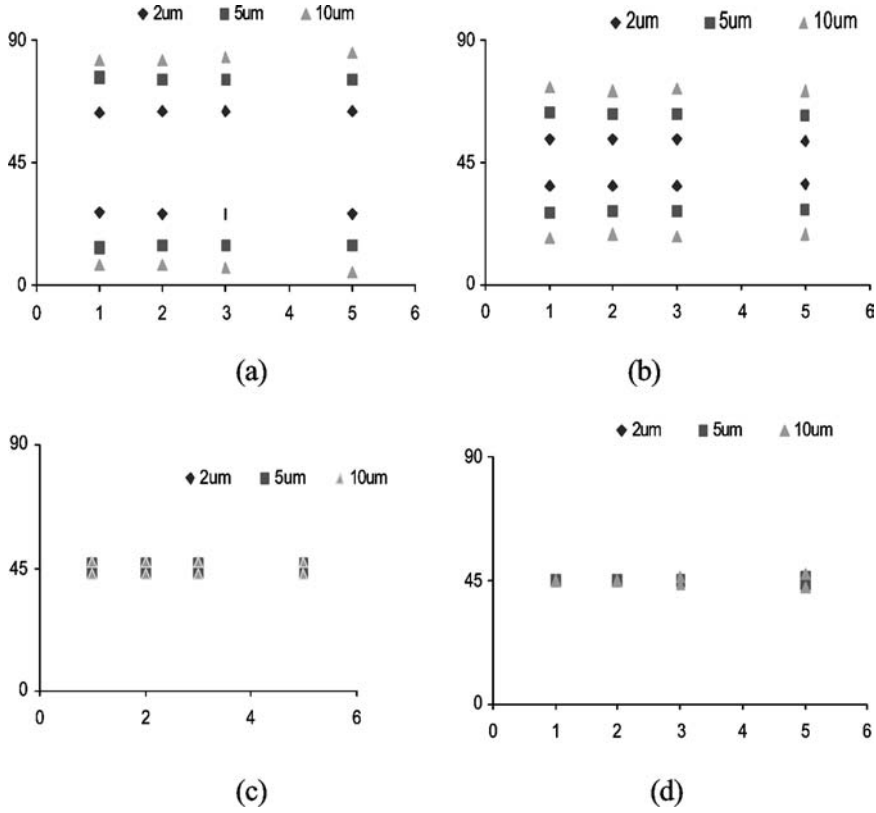

FIGURE 5 Numerical results for different molar extinction coefficient liquid crystal matrices (a) $\varepsilon_{LC} = 300$ (b) $\varepsilon_{LC} = 120$ (c) $\varepsilon_{LC} = 10$ (d) $\varepsilon_{LC} = 0\,m^3/mol/m$.

5. EVANESCENT OPTICAL WAVE STUDIES

An attempt was made to observe the PN distribution directly using evanescent thin film optics. 2 μm cells were processed with a high refractive index prism (SF11) on one side and a normal glass plate (BK7) on the other side as in Figure 6. Both surfaces were coated with PVA and rubbed to produce alignment with a low pretilt angle. The cells were then filled with different concentration PN/PI/LC mixtures. Because of total UV absorption by the prism, the cells had to be exposed through the BK7 plate.

The experimental set up was as described in Figure 7. Above the LC nematic-isotropic transition temperature, the PN is still slightly birefringent producing some depolarisation of the 632.8 nm He-Ne laser, which was measured as a function of the incident angle θ. Close to the critical

Downloaded by [University of California, San Diego] at 10:35 11 August 2012

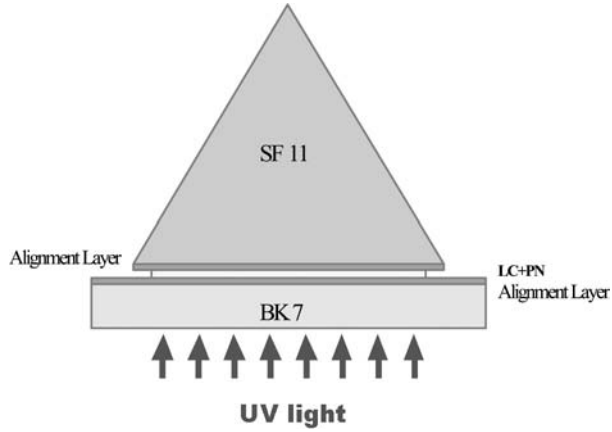

FIGURE 6 Evanescent optical wave cell processing.

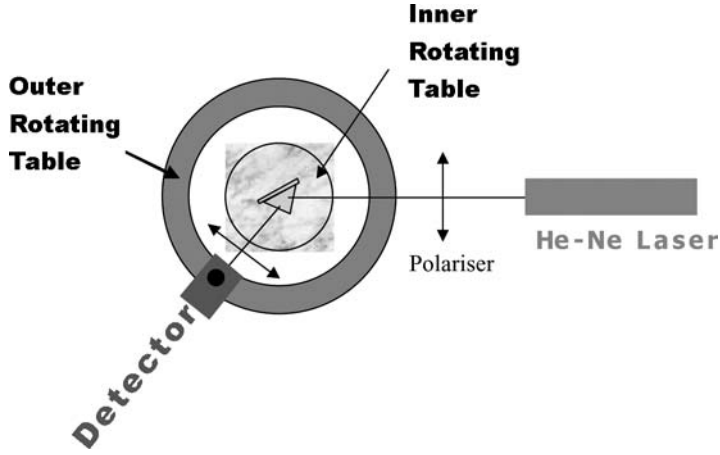

FIGURE 7 Evanescent optical wave experimental method.

angle θ_c, the evanescent field in the cell extends over a distance dependent on the angle θ and the angular dependent depolarisation gives information on the depth dependence of the PN.

The depolarisation detected was unfortunately too low for reliable conclusions to be made on the PN distribution. This was mainly due to the low resulting birefringence of a 5% RM mixture in an isotropic LC, but also to the high concentration of network being formed on the opposite

Downloaded by [University of California, San Diego] at 10:35 11 August 2012

side of the observed surface. The depolarisation measured did not allow proper fitting to the large number (∼50) parameters necessary to describe this 7-layer system. The numerical calculation of the resulting optics was done following the Ko and Sambles [16] 4*4 matrix approximation of the Berreman method [17].

6. CONCLUSIONS

We have developed a model for the formation of polymer networks in liquid crystal cells and compared the resulting predictions with optical observations using absorbing and non-absorbing liquid crystal matrices. This model takes into account the light intensity profile, the rate of polymerisation and molecular diffusion. Both numerical and experimental results agree that UV absorbing LC hosts produce non-uniform PN distributions.

REFERENCES

[1] Dessaud, N. & Raynes, E. P. (2002). *Liq. Crystals*, *29*, 391.
[2] Dessaud, N., Raynes, E. P., & Walton, H. G. (2001). *SID'01 Digest*, 862.
[3] Hikmet, R. A. M. (1996). *Liquid Crystals in Complex Geometries*. In: Crawford (Ed.), Taylor & Francis.
[4] Li, J., Hoke, C., Fredley, D. S., & Bos, P. J. (1996). *SID'96 Digest*, 265.
[5] Hoke, C. D. (1998). *IDW'98 Proceeding*.
[6] Ma, R. Q. & Yang, D. K. (2000). *Phys. Rev. E*, *61*, 1567.
[7] Zhao, G. & Mouroulis, P. (1994). *J. Mod. Opt.*, *41*, 1929.
[8] Bowley, C. C. & Crawford, G. P. (2000). *Appl. Phys. Lett.*, *76*, 2235.
[9] Colvin, V. L., Larson, R. G., Harris, A. L., & Schilling, M. L. (1997). *J. Appl. Phys.*, *81*, 5913.
[10] Qian, T., Kim, J. H., Kumar, S., & Taylor, P. L. (2000). *Phys. Rev. E*, *61*, 4007.
[11] Parker, D. B. V. (1974). *Polymer Chemistry*, Applied Science Publishers Ltd, Ch. 2.
[12] Decker *et al. Photopolymerization: Fundamentals and Applications*, ACS symposium series 673. Scranton, A. B. *et al.* (Ed.), Ch. 6, 63.
[13] Zumer, S. (1996). *Liquid Crystal in Complex Geometries*. In: Crawford, G. P. (Ed.), Taylor & Francis.
[14] Sandler, S. R., Karo, W., Bonesteel, J. A., & Pearce, E. M. (1998). *Polymer Synthesis and Characterization*, Harcourt Publishers Ltd.
[15] Jones, R. C. (1941). *J. Opt. Soc. Am.*, *31*, 488.
[16] Ko, D. Y. K. & Sambles, J. R. (1988). *J. Opt. Soc. Am.*, *5*, 1863.
[17] Berreman, D. W. (1972). *J. Opt. Soc. Am.*, *62*, 502.

Downloaded by [University of California, San Diego] at 10:35 11 August 2012